JOURNAL OF GEOPHYSICAL RESEARCH, VOL. 99, NO. A4, PAGES 5903–5914, APRIL 1, 1994

The proton cyclotron instability and the anisotropy/β inverse correlation

S. Peter Gary,[1] Michael E. McKean,[1,2] Dan Winske,[1] Brian J. Anderson,[3]
Richard E. Denton,[4] and Stephen A. Fuselier[5]

Abstract. Spacecraft observations in the strongly compressed subsolar magnetosheath show an inverse correlation between the proton temperature anisotropy ($T_{\perp p}/T_{\parallel p} > 1$ where $\perp$ and $\parallel$ denote directions perpendicular and parallel to the background magnetic field) and the parallel proton β ($\beta_{\parallel p}$). This manuscript uses one-dimensional hybrid simulations of the proton cyclotron anisotropy instability in homogeneous electron-proton plasmas to study this correlation which may represent a limited closure relation for fluid theories of anisotropic space plasmas. The emphasis is on driven simulations which increase the temperature anisotropy by periodically reducing the magnetic-field-aligned velocities of the protons. The late-time states from ensembles of both initial value and driven simulations yield very similar expressions for the proton anisotropy/$\beta_{\parallel p}$ inverse correlation, and provide a basis for explaining differences between sheath observations from different spacecraft. The driven simulations also yield expressions for the maximum instability growth rate and the fluctuating field energy as functions of $\beta_{\parallel p}$ and a parameter characterizing the anisotropy driver.

1. Introduction

Theoretical models of space plasmas often may be categorized as either macroscopic or microscopic. Macroscopic models, among which single-fluid magnetohydrodynamics (MHD) is a popular example, describe the plasma in terms of locally averaged quantities such as the density, flow velocity, and temperature; these quantities are functions of position and time. Microscopic models are based on kinetic theories such as the Vlasov equation and describe the plasma in terms of distribution functions which are functions of particle velocity as well as position and time.

Computer simulations of large space plasma systems are usually macroscopic in nature and require closure conditions to reduce the number of model equations to a finite, tractible number. These closure conditions often correspond to assumptions such as isotropicity and adiabaticity, conditions which may be useful for collision-dominated fluids but which are not necessarily appropriate for the collisionless plasmas of space. Spacecraft observations often demonstrate distribution functions that are clearly non-Maxwellian, implying that Vlasov theory may be an appropriate mechanism for determining closure under some circumstances [e.g., *Feldman et al.*, 1973, 1976].

If the plasma is sufficiently homogeneous, sufficiently anisotropic, and its anisotropy can be expressed in terms of a macroscopic variable or variables, kinetic theory and simulations may yield a closure relation. The microscopic picture is that plasma instabilities grow in the presence of a strong plasma anisotropy; the associated enhanced fluctuations scatter the particles so as to reduce that anisotropy. *Manheimer and Boris* [1977] argued that, if a macroscopic driving force continually pushes the plasma toward increased anisotropy, the microscopic action to reduce this anisotropy can lead to a relatively steady state balance which corresponds to the instability threshold. Then, for relatively homogeneous space plasmas, this threshold represents a limited closure model for the truncation of the fluid equations.

Manheimer and Boris [1977] also pointed out that linear theory plays a primary role in this process; it is used to identify the appropriate instability and to characterize its threshold in terms of macroscopic parameters. Secondly, kinetic simulations and nonlinear theory may be used to verify that, if a plasma instability is excited, the associated wave-particle interactions move plasma conditions toward threshold and to provide more complete understanding of the physics. But traditional nonlinear exercises such as the

[1]Los Alamos National Laboratory, Los Alamos, New Mexico.
[2]Now at Department of ECE, University of California, San Diego.
[3]Applied Physics Laboratory, Johns Hopkins University, Laurel, Maryland.
[4]Dartmouth College, Hanover, New Hampshire.
[5]Lockheed Palo Alto Research Laboratory, Palo Alto, California.

Paper number 93JA03583.
0148-0227/94/93JA-03583$05.00

calculation of fluctuating field amplitudes and "anomalous" transport expressions play a tertiary role in this procedure.

We use the term "limited closure" to describe a relationship among macroscopic parameters which is induced by microinstability activity. The adjective "limited" implies that such a relation is not valid under all conditions, but that it represents only a bound for the parameter of concern. If the parameter exceeds this bound, the instability is excited and wave-particle scattering returns this parameter to its threshold value, whereas if this limit is not exceeded, there is no instability growth, no scattering, and no change in the parameter value.

Closure relations from instabilities are limited in another sense. Collisionless plasmas are subject to a variety of free energies or anisotropies which correspond to a variety of microinstabilities [*Gary*, 1993] which, in turn, imply a variety of threshold conditions. This implies a diversity of closure relations for macroscopic parameters, each of which contributes to but does not necessarily complete the process of closing a set of fluid model equations. For example, in the case considered here the threshold condition for the proton cyclotron anisotropy instability implies a relationship between the proton temperature anisotropy $T_{\perp p}/T_{\parallel p}$ and $\beta_{\parallel p}$. (Here $\parallel$ and $\perp$ denote directions parallel and perpendicular to the background magnetic field $\mathbf{B}_o$, respectively.) This relationship can be used to determine one macroscopic variable, say $T_{\perp p}$, but closing of the equation for $T_{\parallel p}$ requires further information, such as might be provided by an equation of state or by a heat flux limitation. Our analysis assumes that the heat flux is zero; if a limit on the heat flux would be observed to exist, it would be determined by quite different threshold conditions associated with quite different heat flux instabilities [e.g., *Feldman et al.*, 1976].

To date, no collisionless microscopic theory has provided a widely accepted prescription for limited closure of a macroscopic space plasma model. One reason for this is the variety of anisotropies and associated thresholds possible in space plasmas. Another reason is that microinstabilities do not operate uniformly throughout space but, rather, assert themselves only locally and sporadically. Thus it is necessary to distinguish between parcels of plasma that are "active" and "inactive."

If macroscopic changes in the system cause a species distribution within a plasma parcel to become sufficiently anisotropic so that a microinstability is excited, field fluctuations will become enhanced, and wave-particle scattering due to those enhanced fluctuations will act to reduce the anisotropy. If a balance between macro- and microprocesses is established, the anisotropy is maintained near instability threshold, and we term that plasma parcel to be active. By this definition, if a spacecraft were to pass through such a parcel, it would observe both field fluctuation spectra that indicated instability growth and dimensionless plasma parameters that satisfied the instability threshold condition. If macroscopic forces do not lead to instability growth within a plasma parcel, we term that parcel inactive. In such a case, spacecraft observations might show evidence of either characteristic enhanced fluctuations or satisfaction of a threshold condition but not both. In inactive plasma parcels, the anisotropy might be observed to have many possible values up to (but not beyond) its value at threshold. In this latter case, which appears to be the predominant state of many near-Earth space plasmas, there is no compelling evidence that the plasma is maintained at threshold.

The purpose of this manuscript is to use linear theory and hybrid computer simulations to examine the specific case of the proton temperature anisotropy threshold of the proton cyclotron anisotropy instability and to relate our simulation results to observations in the terrestrial magnetosheath. The use of this threshold as a limited closure relation for an anisotropic fluid model has been considered elsewhere [*Denton et al.*, 1994b]. The basic model, which we use for both our theory and simulations, is a simple one: We consider a homogeneous electron-proton plasma with an initially bi-Maxwellian proton distribution function with $T_{\perp p}/T_{\parallel p} > 1$. Such an anisotropy has been observed frequently in the magnetosheath [*Tsurutani et al.*, 1982; *Sckopke et al.*, 1990; *Anderson et al.*, 1991; *Farris et al.*, 1993] and can excite several different instabilities there [*Gary et al.*, 1976].

Recent observations [*Anderson and Fuselier*, 1993; *Anderson et al.*, 1994] and linear theory [*Gary et al.*, 1993a] have demonstrated that the proton cyclotron anisotropy instability has the larger growth rate and dominates magnetic fluctuation spectra at $\beta_{\parallel p} \lesssim 1$ in the magnetosheath, whereas the mirror instability may have the larger growth rate and certainly dominates the fluctuation properties at higher β values. Yet the identification of enhanced fluctuations from a particular instability in either spacecraft data or computer simulations does not necessarily imply that that instability plays an important role in determining the properties of the plasma. Simulations [*McKean et al.*, 1992b, 1994] have shown that, even at relatively high β, the mirror instability is not as effective at reducing proton anisotropies as is the proton cyclotron instability under typical magnetosheath conditions. Therefore we consider only the latter growing mode in the following development. Section 2 reviews some appropriate results of the linear theory of this instability and emphasizes that different values of the maximum growth rate γ_m correspond to different threshold conditions.

Anderson and Fuselier [1993] used observations from the Active Magnetospheric Particle Tracer Explorer/Charge Composition Explorer (AMPTE/CCE) spacecraft to study the subsolar sheath downstream of quasi-perpendicular bow shocks during times at which the magnetosphere was strongly compressed by the solar wind. These authors carried out a statistical study which showed that the proton anisotropies, which typically satisfy the condition $T_{\perp p}/T_{\parallel p} > 1$ in the sheath, exhibited a relatively small variation for a given value of $\beta_{\parallel p}$ and that the data were consistent with an inverse correlation between the proton anisotropy and the proton $\beta_{\parallel}$. This was stated by *Anderson et al.* [1994] as

$$\frac{T_{\perp p}}{T_{\parallel p}} - 1 = \frac{0.85}{\beta_{\parallel p}^{0.48}} \tag{1}$$

where $\beta_{\parallel p} \equiv 8\pi n_p T_{\parallel p}/B_o^2$ (see Appendix II of *Anderson et al.* [1994] for the different definitions of β_p used in this and related papers), and the range of observed $\beta_{\parallel p}$ was $0.02 \lesssim \beta_{\parallel p} \lesssim 10.0$. A similar result has been found in the AMPTE/CCE data from the subsolar magnetosheath downstream from quasi-parallel shocks for $1.0 \lesssim \beta_{\parallel p} \lesssim 30.0$ [S. A. Fuselier, Private Communication]. These observations have the same form as the theoretical thresholds of

ion cyclotron aniostropy instabilities [*Gary et al.*, 1993c], suggesting that under certain conditions plasma parcels in the magnetosheath may be active to these instabilities and that, as a result, the threshold condition may manifest itself in the data.

Somewhat different results have been obtained by *Phan et al.* [1994] in a statistical study of magnetosheath data from the AMPTE/Ion Release Module (AMPTE/IRM) spacecraft which sampled a much wider range of sheath parameters. Their data points show a much greater variation in $T_{\perp p}/T_{\|p}$ at a given $\beta_{\|p}$ and appear to be bounded above by equation (1) [*Hau et al.*, 1993]. *Phan et al.* [1994] report a best fit to their data of

$$\frac{T_{\perp p}}{T_{\|p}} - 1 = \frac{0.58}{\beta_{\|p}^{0.53}} \tag{2}$$

Section 3 provides an interpretation of the differences between equation (1) and equation (2).

Gary and Winske [1993] and *Denton et al.* [1993] used hybrid simulations to show that wave-particle scattering maintains the proton anisotropy near cyclotron instability threshold. *Gary et al.* [1993c] further used hybrid simulations to show that these instabilities lead both proton and helium ions to satisfy threshold conditions similar to equation (1) in the magnetosheath. The sum of these linear and simulation results provides strong evidence that ion cyclotron anisotropies instabilities are indeed the physical mechanism leading to the observed ion anisotropy/$\beta_{\|p}$ inverse correlations, and that these correlations are fundamental properties of plasmas in which such instabilities are active.

Yet many questions remain to be answered concerning this topic. In this manuscript we address two of these questions: (1) Can simulations emulate the differences between the CCE and IRM proton anisotropy observations? and (2) Among the many different thresholds for a particular instability, can simulations determine the condition appropriate for a given plasma regime?

Section 3 of this manuscript uses initial value hybrid simulations to address the first question, and the remainder of this manuscript describes research with driven simulations directed toward answering the more difficult second question. Most of our recent simulations [*McKean et al.*, 1992b; *Gary and Winske*, 1993; *Gary et al.*, 1993c] have been initial value computations of an isolated system; after the ions were given an initial anisotropy, the system was permitted to evolve in time without further interference. In contrast, the active magnetosheath may represent a system in which the proton anisotropy of a plasma parcel is continually sustained by large-scale effects such as magnetic compression perpendicular to the magnetic field and extension or stretching parallel to the field as the sheath plasma is pressed against the magnetospheric obstacle [*Denton et al.*, 1994b].

Thus in sections 4 and 5 we study driven hybrid simulations in which the parallel velocities of individual superparticles are periodically changed in order to emulate a macroscopic process which attempts to continually increase the anisotropy of the ion distribution functions. The growth of ion cyclotron anisotropy instabilities and the consequent reduction of the ion $T_\perp/T_\|$ by wave-particle scattering balances the anisotropy enhancement so that at sufficiently late times a relatively constant value of the anisotropy emerges which corresponds to a maximum instability growth rate γ_m. We find that late-time results from an ensemble of such simulations yield not only an anisotropy/β relation similar to those obtained by observations, linear theory, and initial value simulations but also expressions for the $\beta_{\|p}$ dependence of the maximum instability growth rate and the fluctuating field energy density. In section 6 we synthesize our results; section 7 discusses the limitations of this work and the implications of our results for future observational studies of the terrestrial magnetosheath.

With one exception our notation is the same as in our recent papers on this subject [*Gary et al.*, 1993a, b, c; *Gary and Winske*, 1993]; the exception is $\beta_{\|p}$ where, as noted above, we define this quantity in terms of the proton density. We assume an electron-proton plasma throughout and defer consideration of the effects of magnetosheath helium to other manuscripts.

2. Linear Theory and Instability Thresholds

It is now well established that the threshold condition for the proton cyclotron anisotropy instability represents an inverse correlation between $T_{\perp p}/T_{\|p}$ and $\beta_{\|p}$ similar to that observed in the sheath [*Gary et al.*, 1993c]. This section restates the idea that there are many different thresholds for this instability, corresponding to different values of the maximum growth rate γ_m [*Gary et al.*, 1976] and for the first time provides a closed-form best fit expression to these thresholds for three values of γ_m.

Two primary types of enhanced fluctuations are observed in the magnetosheath at frequencies below Ω_p: mirror-like fluctuations [*Tsurutani et al.*, 1982; *Lacombe et al.*, 1992; *Song et al.*, 1992, and references therein] and proton-cyclotron-like fluctuations [*Sckopke et al.*, 1990; *Takahashi et al.*, 1991; *Anderson et al.*, 1991; *Lacombe et al.*, 1992; *Anderson and Fuselier*, 1993; *Farris et al.*, 1993]. The most frequent theoretical interpretation of these observations is that they are due to the growth of the mirror and proton cyclotron instabilities driven by the anisotropy of a single proton component with $T_{\perp p}/T_{\|p} > 1$ [*Gary et al.*, 1993a, and references therein]. The reflected proton component may also contribute to excitation of an electromagnetic ion/ion instability [*Brinca et al.*, 1990] or an ion ring instability at harmonics of Ω_p [*Dendy and McClements*, 1993], and the anisotropic helium ions in the sheath may lead to growth of the helium cyclotron anisotropy instability [*Gary et al.*, 1993a; *Denton et al.*, 1993, 1994a]. There is also the possibility of enhanced magnetic fluctuations driven by magnetic field shear and the density gradient near the magnetopause [*Song et al.*, 1993; *Anderson and Fuselier*, 1993] .

We here concentrate on the proton cyclotron anisotropy instability, because both computer simulations [*McKean et al.*, 1992b, 1994] and the correlation of theory with CCE data analysis [*Gary et al.*, 1993c] have demonstrated that it should be the strongest contributor to the proton anisotropy/β inverse correlation under typical active magnetosheath conditions. Because the maximum growth rate of this instability corresponds to $\mathbf{k} \times \mathbf{B}_o = 0$ [*Gary et al.*, 1976], we consider here and throughout this manuscript only the case of propagation parallel to the background magnetic field.

We also consider for the theory and simulations the case of a spatially homogeneous background plasma. This approximation will be valid as long as the wavelength of fluctuations of concern are very small compared to the inhomogeneity scale length along $\mathbf{B}_o$ which we denote by $L_\parallel$. The characteristic wavenumber of the proton cyclotron anisotropy instability is $kc/\omega_p \simeq 0.50$; for a proton density of order 100 cm^{-1} [*Anderson and Fuselier*, 1993] this corresponds to a wavelength of about 300 km, far smaller than the *Denton et al.* [1993] estimate of $L_\parallel \simeq 16{,}000$ km.

Although terminology varies with different authors, we here define our use of the terms "marginal stability" and "instability threshold." The marginal stability condition of a growing mode is a unique value of the parameter characterizing the anisotropy or free energy such that $\gamma \leq 0$ for all wavenumbers but such that a small increase in this parameter leads to $\gamma > 0$ at some wavenumber. This marginal condition, however, corresponds to infinitesimally slow fluctuation growth and is not useful in most real plasmas where an instability must have a growth rate substantially greater than the rate of macroscopic plasma change if it is to assert itself. We define "instability threshold" to correspond to the value of the anisotropy parameter such that the maximum growth rate of a growing mode corresponds to a given nonzero value. For example, the results of *Gary et al.* [1993c] suggest that $\gamma_m = 0.01\Omega_p$ implies an appropriate threshold for the proton cyclotron anisotropy instability in the highly compressed magnetosheath. But more generally, a threshold may correspond to any nonzero value of the maximum growth rate; since our concern here is with a variety of possible applications, we consider a range of γ_m values and a corresponding range of threshold conditions.

The discrete symbols of Figure 1 show the proton anisotropy as a function of $\beta_{\parallel p}$ obtained from linear Vlasov theory for three different maximum growth rates of the proton cyclotron anisotropy instability. These three types of

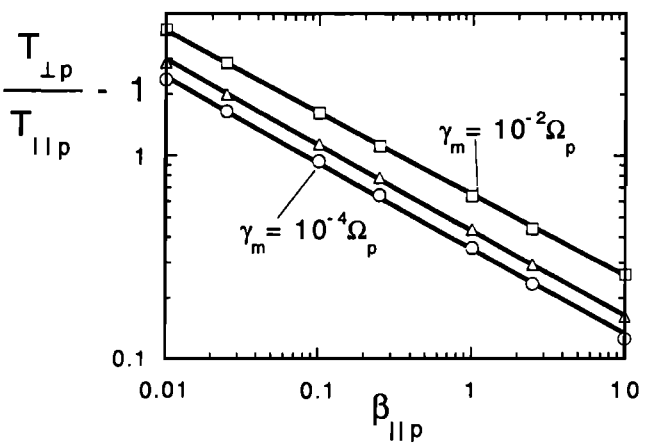

Figure 1. The proton temperature anisotropy as a function of $\beta_{\parallel p}$ for the proton cyclotron anisotropy instability. The model used here and in all the figures of this manuscript is a two-species plasma of electrons and protons. Here the electrons are isotropic, $T_{\parallel e}/T_{\parallel p} = 0.25$, and $v_A/c = 10^{-4}$. The arrays of open squares, triangles, and circles represent results from linear Vlasov theory corresponding to $\gamma = 10^{-2}\Omega_p$, $10^{-3}\Omega_p$, and $10^{-4}\Omega_p$, respectively. The three solid lines represent the best fits to each array, corresponding to equation (3).

symbols correspond to three threshold curves of Figure 3 of *Gary et al.* [1976]; here we extend that early work and do least squares fits to the theoretical results. Such fits are shown as the three solid lines in Figure 1; they correspond to the following expressions:

$$\frac{T_{\perp p}}{T_{\parallel p}} - 1 = \frac{0.35}{\beta_{\parallel p}^{0.42}} \qquad (\gamma_m = 10^{-4}\Omega_p) \qquad (3a)$$

$$\frac{T_{\perp p}}{T_{\parallel p}} - 1 = \frac{0.43}{\beta_{\parallel p}^{0.42}} \qquad (\gamma_m = 10^{-3}\Omega_p) \qquad (3b)$$

$$\frac{T_{\perp p}}{T_{\parallel p}} - 1 = \frac{0.65}{\beta_{\parallel p}^{0.40}} \qquad (\gamma_m = 10^{-2}\Omega_p) \qquad (3c)$$

Note that, although the numerators on the right-hand sides of these equations vary with growth rate, the power of $\beta_{\parallel p}$ does not change significantly among the three examples. Yet both observations [equation (1)] and simulations (see below) typically yield larger values of this exponent at threshold. Our discussions below will illuminate some of the reasons for this difference.

3. Initial Value Simulations

The one-dimensional hybrid code of *Winske and Omidi* [1993] has been used many times to simulate the proton cyclotron anisotropy instability [*McKean et al.*, 1992b; *Gary et al.*, 1993b, 1993c; *Gary and Winske*, 1993]. In each of these papers, only active plasmas were considered; that is, the simulations began with ion anisotropies well above cyclotron instability thresholds so that strong fluctuation growth was excited and the anisotropies were reduced toward threshold by wave-particle scattering. However, many space plasmas are inactive; if, for example, ion anisotropies are initially below threshold of the anisotropy instabilities, those modes will not grow and there will be little change in that free energy. Although the latter such cases are uninteresting theoretically, they are often present in the data, and it is useful to include such cases in our ensemble of simulations to facilitate comparison with the observations. *Anderson* [1993] has already drawn the distinction between active and inactive observations in the CCE data from Earth's magnetosphere.

We have carried out an ensemble of initial value simulations of the proton cyclotron anisotropy instability for both active and inactive conditions. Results from this ensemble are illustrated in Figure 2 which once again shows the proton anisotropy as a function of $\beta_{\parallel p}$. The top panel of Figure 2 illustrates the initial conditions, whereas the bottom panel shows the same parameters at the end of our simulations at $\Omega_p t = 200$. Our initial conditions were chosen so as to give a broad distribution of initial points across the proton anisotropy-$\beta_{\parallel p}$ plane and to include both active cases (the solid symbols) as well as inactive simulations (the open symbols). Here our (somewhat arbitrary) criterion for distinguishing these two categories is that active runs correspond to an initial value of $\gamma_m \geq 10^{-3}\Omega_p$, whereas the opposite category corresponds to the opposite sense of the inequality. In terms of the dimensionless fluctuating magnetic field energy density $\epsilon/\epsilon_o \equiv |\delta\mathbf{B}|^2/B_o^2$, the active runs typically satisfied the empirical condition $0.004\,\beta_{\parallel p} < (\epsilon/\epsilon_o)$ sometime during the simulation, whereas the inactive simulations typically satisfied $(\epsilon/\epsilon_o) < 0.004\beta_{\parallel p}$ throughout the run.

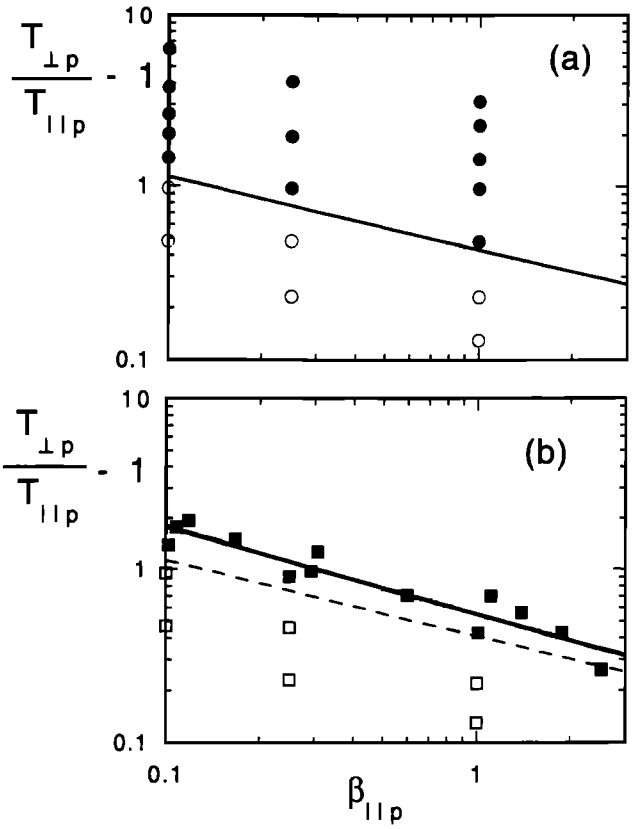

Figure 2. The proton anisotropy from an ensemble of initial value simulations of the proton cyclotron anisotropy instability as a function of $\beta_{\|p}$. (a) The anisotropy and $\beta_{\|p}$ at $t = 0$ from each simulation. (b) The corresponding values at $\Omega_p t = 200$. The solid symbols represent results from active simulations in which the initial maximum growth rate satisfied $\gamma_m > 10^{-3}\Omega_p$. The open symbols show results from inactive simulations; that is, the initial maximum growth rate met the condition $\gamma_m < 10^{-3}\Omega_p$. The solid line in (a) represents the linear theory threshold result corresponding to $\gamma = 10^{-3}\Omega_p$ [equation (3b)]. The solid line in (b) represents the least squares fit to the results from the active simulations, equation (4), whereas the dashed line corresponds to the best fit for the entire ensemble of simulation results, $T_{\perp p}/T_{\|p} - 1 = 0.41/\beta_{\|p}{}^{0.44}$.

It is clear that the active cases uniformly suffer reductions in proton anisotropies. The late-time parameters for these simulations typically correspond to growth rates which fall in the range $10^{-3} \lesssim \gamma_m \lesssim 2.5 \times 10^{-2}$. A least squares fit to the late-time anisotropies for the active runs yields

$$\frac{T_{\perp p}}{T_{\|p}} - 1 = \frac{0.55}{\beta_{\|p}{}^{0.51}} \tag{4}$$

with a linear correlation coefficient $R = 0.94$. The coefficient of 0.55 appropriately stands between the corresponding coefficients of equations (3b) and (3c), but the exponent of 0.51 is somewhat larger than any of the exponents of equations (3a) through (3c). The latter result reflects the fact that in our ensemble of active simulations the higher β runs correspond, on average, to smaller values of γ_m, thus implying a small increase in the slope of the fit as compared to the linear theory fits which are for constant γ_m at all $\beta_{\|p}$ values. We will study this effect in more detail shortly.

In contrast, the simulations of inactive plasmas for the most part undergo relatively small changes in $T_{\perp p}/T_{\|p}$ [*Denton et al.*, 1993, Figure 9]. There is no physics in the late-time anisotropy versus β distribution of these runs, because one may obtain almost any result by an appropriate choice of initial conditions. However, it is clear that if one adds together results from the two ensembles, a best fit to the anisotropies will probably change the exponent of $\beta_{\|p}$ and will certainly yield a smaller coefficient than a fit to the active results alone. For example, the best fit to all the points of Figure 2 yields $T_{\perp p}/T_{\|p} - 1 = 0.41/\beta_{\|p}{}^{0.44}$ with $R = 0.67$.

This analysis provides at least a partial explanation for the differences between the CCE observations [e.g., equation (1)] and the IRM observations [equation (2)]. Because the CCE spacecraft traversed the magnetosheath only under highly compressed magnetospheric conditions, it is likely that the observations of *Anderson et al.* [1994] corresponded to active plasmas which were maintained close to instability threshold by wave-particle scattering. On the other hand, IRM crossed the magnetosheath under a much wider variety of conditions, many of which presumably led to the observation of plasmas that were inactive. Thus, as in Figure 2, many of the data points of *Phan et al.* [1994] may lie well below the threshold condition and, as in Figure 2, a fit to their data will yield a relationship which lies well below the fits obtained from CCE.

There are several additional possible sources for the difference between the fits to the CCE and IRM observations. These sources include magnetic shear at the magnetopause [*Anderson and Fuselier*, 1993; *Song et al.*, 1993; *Phan et al.*, 1994], solar wind dynamic pressure and associated compression of the magnetosheath/magnetosphere [*Anderson and Fuselier*, 1993], cone angle of the interplanetary magnetic field [S. A. Fuselier, Private Communication], and helium ion concentration [e.g., *Gary et al.*, 1993a]. Because both data sets contained a variety of different magnetopause shear conditions, only the latter three sources need to be considered.

The He^{++} particle density observed in the magnetosheath by CCE was about 4% of the corresponding n_p [*Fuselier et al.*, 1991a], a value typical of that in the solar wind. There is no reason to think that the helium density was much different during the IRM observations because the two data sets partially overlap in time and the IRM data set is sufficiently large so as to represent an essentially random sample of solar wind conditions. Therefore differences in magnetosheath helium densities are not a likely source of the CCE/IRM difference.

The remaining two effects both may affect local sheath conditions in ways which contribute to the difference between equation (1) and equation (2). The CCE observations were for uniformly high solar wind dynamic pressure and were restricted to large IMF cone angles [*Anderson et al.*, 1994], whereas the IRM observations corresponded on average to more normal dynamic pressure and a wider range of IMF cone angles [*Phan et al.*, 1994]. A more detailed understanding of how these external factors affect local conditions must await further data analysis. Here we note only that differences in the solar wind dynamic pressure, especially, may bias the CCE data set toward more active sheath conditions and the IRM data toward more in-

active plasmas. This interpretation is consistent with the result that the IRM data fit of equation (2) lies below the threshold condition of the CCE data fit [equation (1)].

It is important to note that this interpretation applies only to averages of the data sets. For data from an individual spacecraft pass through the magnetosheath, all the factors mentioned above may influence the anisotropy/β relationship.

In summary, our initial value simulation results support the interpretation that equation (1), the anisotropy/$\beta_{\|p}$ correlation observed from the CCE spacecraft, approximately corresponds to an instability threshold condition, whereas equation (2), the correlation observed from IRM, represents a broader spectrum of plasma conditions. Therefore, although both sets of observations are likely to be valid and contribute to our understanding of magnetosheath processes, the CCE results better indicate the physics leading to the anisotropy/β inverse correlation.

4. Driven Simulations: The Model

In this section we discuss the relationship between macroscopic sheath processes acting to make the ions more anisotropic and the simulation algorithm we have chosen to emulate these processes. If the timescale for action of such macroscopic processes is no faster than the time for a plasma parcel to transit the subsolar magnetosheath, these processes have no significant effect. In contrast, if the characteristic frequency of such processes is greater than the proton cyclotron frequency, the protons are so strongly perturbed that the instability cannot grow [*Denton et al.*, 1993, Figure 7]. However, if the macroscopic driver has a characteristic rate which can be matched by wave-particle scattering , then a balance between the two can be established, a quasi-steady condition may prevail at an instability threshold, and the plasma may be maintained in the active state defined above. This is the essence of the marginal stability analysis advocated by *Manheimer and Boris* [1977].

An "instability can only be important for long periods in a steady state plasma if some external...mechanism continually drives the system toward instability" [*Manheimer and Boris*, 1977, p. 16]. The primary macroscopic effect which appears to drive the anisotropy in the magnetosheath is the draping of magnetic field lines against the magnetosphere; *Denton et al.* [1994b] have argued that the anisotropy increase is due to a combination of magnetic compression increasing $T_{\perp p}$ and magnetic-field-line stretching which decreases $T_{\|p}$. Because it is difficult to represent either of these effects in our one-dimensional simulations, we have chosen to model anisotropy driving by a numerical algorithm which periodically reduces the $v_{\|}$ of simulation superparticles. On the microscopic side, "the primary effect of wave-particle interactions due to a particular instability is to reduce the souce of free energy driving that instability" [*Gary*, 1980, p.1193]. Here, as we have discussed above, we assume that the particular growing mode of concern is the proton cyclotron anisotropy instability; the primary nonlinear consequence of the growth of this mode is, of course, the reduction of $T_{\perp p}/T_{\|p}$.

To model the driven increase in proton anisotropy in the sheath, we have used a recycle algorithm which periodically changes velocities of individual superparticles. These one-dimensional hybrid simulations, which utilize the code described by *Winske and Omidi* [1993], are generally similar to the "recycled" simulations of *Ambrosiano and Brecht* [1987] and *McKean et al.* [1992a] or the "refreshed" simulations of *Denton et al.* [1993], but are different in detail.

The simulations of ion cyclotron instabilities by *Denton et al.* [1993] have particular relevance to our driven simulations. These authors defined a refreshment time τ_{ref} which characterized the timescale over which simulation particles had their velocities changed. *Denton et al.* [1993] then showed that fast refreshment rates ($\tau_{ref}\Omega_p \lesssim 10$) prevented instability growth, whereas very slow refreshment rates ($\tau_{ref}\Omega_p \gtrsim 500$) apparently yielded results which were similar to those from initial value simulations. Simulation results at intermediate values of τ_{ref} showed in effect a balance between anisotropy increases by the refreshment processs and anisotropy reduction by wave-particle scattering. A major purpose of the next section is to further explore this balance.

Although we here report results for only one recycling algorithm, we have also done extensive studies with a second, somewhat different particle recycling procedure which has yielded results qualitatively similar to those described below. Both algorithms have the property that ions with relatively large $|v_{\|}|$ are reduced to smaller parallel speeds. These algorithms do not remove particles from the simulation and therefore do not represent either the decreasing plasma density or the increasing magnetic field which are often observed as spacecraft approach the magnetopause [*Song et al.*, 1990; *Fuselier et al.*, 1991b; *Anderson and Fuselier*, 1993; *Song et al.*, 1993; *Paschmann et al.*, 1993]. They do, however, represent the increase in ion anisotropy observed in this region; because the simulations also represent the wave-particle reduction in anisotropy, these computations should provide insight into the competition between macroscopic and microscopic effects in the sheath.

5. Driven Simulations: The Results

In this section we define the recycle process used in our driven simulations. We then examine results from an ensemble of driven simulations of the proton cyclotron anisotropy instability and establish parametric scalings for the late-time values of γ_m and ϵ/ϵ_o.

The recycling process used in our driven simulations periodically reduces the field-aligned speeds of all ions but provides a greater such reduction to those particles with the largest such speeds. For each run we choose a cutoff speed v_{cut}; we always take $v_{cut} >> v_p$ in order to avoid strong perturbations of the thermal protons. Then once every recycle period, $\Delta\tau$, we reduce the field-aligned velocity of each ion, $v_{\|}$, to a new value given by

$$v_{\|new} = v_{\|} \exp\left(-\frac{v_{\|}^2}{v_{cut}^2}\right) \tag{5}$$

The perpendicular components of the ion velocity remain unchanged to minimize the perturbing effects of the recycle process. Here $\Delta\tau = 100\Delta t$ and our simulation time step is $\Delta t\Omega_p = 0.05$. Then the recycle frequency at each time step can be computed as

$$\nu_{rec} = \frac{\Sigma|v_{\|} - v_{\|new}|}{v_A\, \Delta\tau\, N_{total}} \tag{6}$$

where the sum is over all the superparticles, v_A is the Alfvén speed, and N_{total} is the total number of superparticles in the simulation.

If we assume that the reduced proton distribution function in the direction parallel to $\mathbf{B}_o$ remains Maxwellian with an instantaneous temperature $T_{\|p}(t)$, then we may replace the sum over particles in equation (6) with an integral over the parallel velocity component. Then it follows that

$$\frac{\nu_{rec}}{\Omega_p} = \sqrt{\frac{\beta_{\|p}(t)}{\pi}} \frac{1}{\Delta\tau\,\Omega_p} \frac{1}{1 + \frac{v_{cut}^2}{2v_p^2(0)} \frac{T_{\|p}(0)}{T_{\|p}(t)}} \tag{7}$$

or, because $v_{cut} >> v_p$,

$$\frac{\nu_{rec}}{\Omega_p} \simeq \frac{1}{\sqrt{\pi}\Delta\tau\,\Omega_p} \frac{[\beta_{\|p}(t)]^{1.5}}{\beta_{\|p}(0)} \frac{2v_p^2(0)}{v_{cut}^2} \tag{8}$$

Some results from a representative simulation of the proton cyclotron anisotropy instability using this recycling algorithm are presented in Figure 3. After an initial phase in which the system develops its response to the recycling process, the system enters a late-time phase in which the fluctuating magnetic field energy attains saturation, $T_{\perp p}/T_{\|p}$ remains relatively constant, but $\beta_{\|p}$ and ν_{rec}/Ω_p gradually diminish with time. The recycling procedure not only reduces $T_{\|p}$ but removes ion kinetic energy from the system; although pitch angle scattering by the enhanced fluctuations tries to increase this temperature, it is not effective enough to arrest the gradual decrease in $T_{\|p}$. Since n_p and $\mathbf{B}_o$ are constant in these simulations, this decrease translates into the decrease in $\beta_{\|p}$ shown in Figure 3. As for initial value simulations of this instability, there is a gradual transfer of fluctuation energy density from shorter to longer wavelengths [*McKean et al.*, 1992b; *Gary and Winske*, 1993], so that for the (necessarily) limited temporal extent of our runs a fully time-independent asymptotic state is not generally established.

Figure 4 shows proton anisotropy versus $\beta_{\|p}$ results from an ensemble of fifteen driven simulations at both early and late times. Because the initial value of the proton temperature anisotropy is not necessarily the maximum value in these driven simulations (the example of Figure 3 is characteristic of these runs), the solid circles represent the anisotropy values corresponding to the early-time maximum of $T_{\perp p}/T_{\|p}$. The solid squares represent late-time values of the anisotropy from the same runs. Here, as in Figure 5, late-time points are obtained by averaging simulation data over five values corresponding to the times $\Omega_p t'$, $\Omega_p t' \pm 5$, and $\Omega_p t' \pm 10$, at $\Omega_p t' = 250$, 350, and 450 subject to the additional condition that t' is equal or greater than the time of saturation of the total fluctuating magnetic field energy density.

Although the active initial value simulations correspond to proton heating and a consequent increase of $\beta_{\|p}$ (Compare Figures 2a and 2b), it is evident from both Figures 3 and 4 that the driven simulations imply a reduction in the proton parallel β with time. Nevertheless, it is also clear that the microphysics of the two simulation types is the same, because the anisotropy/β relation is so similar in the two cases. The least squares fit of the late-time results of Figure 4 yields

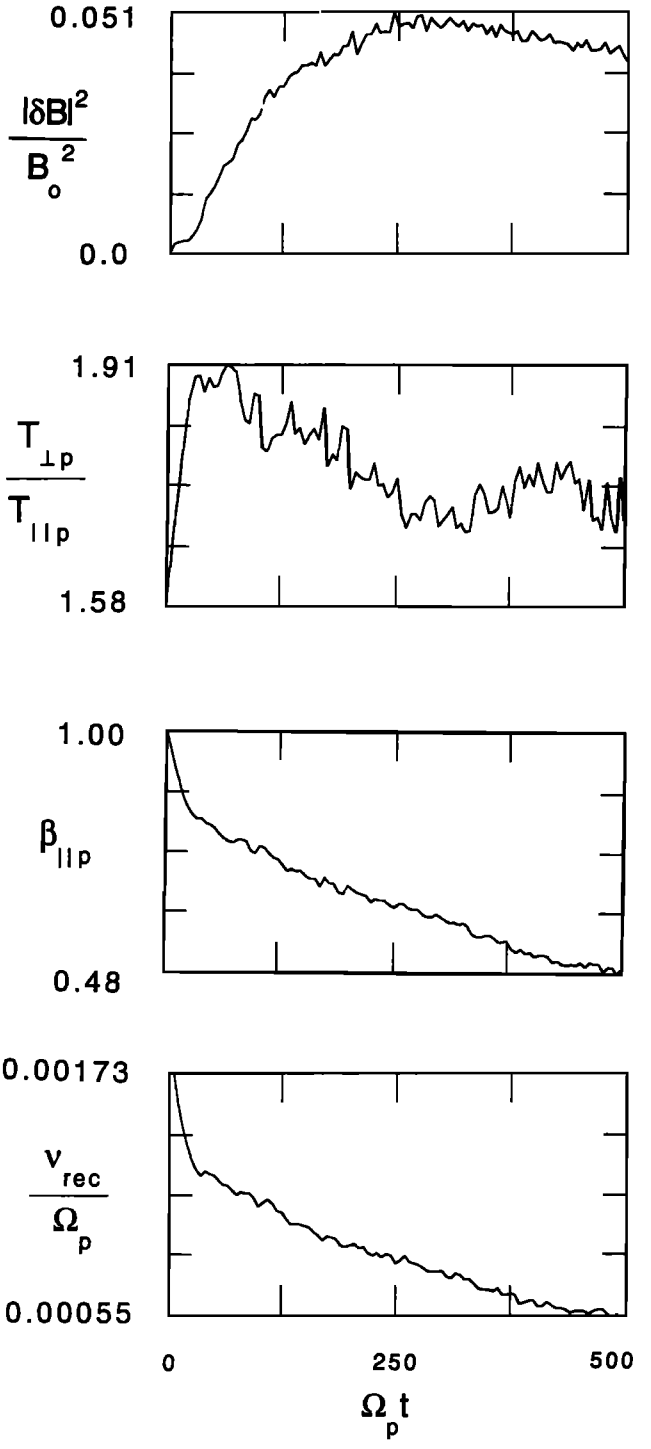

Figure 3. Results from a driven simulation of the proton cyclotron anisotropy instability. The initial parameters here are $\beta_{\|p} = 1.00$ and $T_{\perp p}/T_{\|p} = 1.58$. The cutoff speed is $v_{cut} = 8.0\sqrt{2}v_p$. The four panels here represent the total fluctuating magnetic field energy, the proton temperature anisotropy, the proton parallel β, and the recycle frequency as functions of time.

$$\frac{T_{\perp p}}{T_{\|p}} - 1 = \frac{0.55}{\beta_{\|p}^{0.52}} \tag{9}$$

with a linear correlation coefficient of $R = 0.996$, a result very similar to equation (4) from the late-time initial

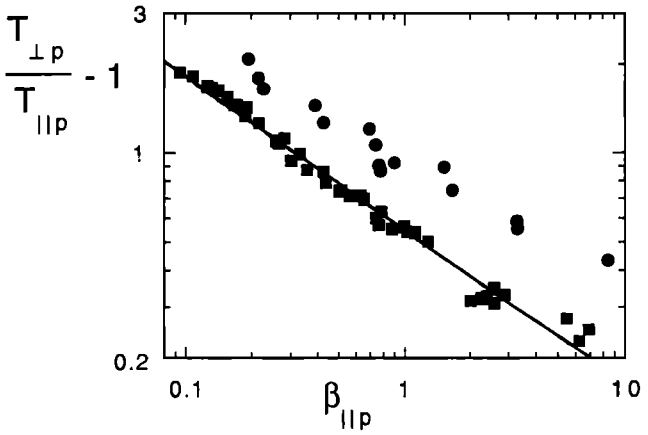

Figure 4. The proton anisotropy from an ensemble of driven simulations of the proton cyclotron anisotropy instability as a function of $\beta_{\|p}$. For this ensemble of runs the initial values of $\beta_{\|p}$ ranged from 0.25 to 10.0; the values of v_{cut} used ranged from 5 $\sqrt{2}v_p$ to 12 $\sqrt{2}v_p$. The solid circles represent the maximum early-time value of the anisotropy from each simulation. The solid squares show the corresponding late-time anisotropies selected and averaged as described in the text. The line represents the least squares fit to the late-time results, equation (9).

value simulations of Figure 2. This similarity is strong evidence that our recycle process does not strongly perturb the plasma and that the same microinstability processes are operating in both the initial value and driven simulations.

The late-time proton temperature anisotropies of our driven simulations are best fit by equation (9); if we do least squares fits as functions of the variable $\beta_{\|p}/(v_{cut}/v_p)^\alpha$ where $\alpha > 0$, the correlation coefficient decreases in magnitude as α increases. This indicates that the anisotropy/β relation is independent of the rate at which the proton cyclotron instability is being driven. In contrast, the late-time maximum growth rate (computed from linear theory using the late-time values of the proton anisotropy and $\beta_{\|p}$) and the late-time fluctuating field energy density are functions of the instability driving rate; if we seek the α values which yield the largest correlation coefficients, we obtain

$$\frac{\gamma_m}{\Omega_p} \simeq 0.0026 \left(\frac{\beta_{\|p}}{(v_{cut}/\sqrt{2}v_p)^{1/2}} \right)^{-0.57} \quad (10)$$

with $R = 0.95$, and

$$\frac{\epsilon}{\epsilon_o} \simeq 1.38 \left(\frac{\beta_{\|p}}{(v_{cut}/\sqrt{2}v_p)^2} \right)^{0.73} \quad (11)$$

with $R = 0.992$. The late-time simulation results as well as these best fits are displayed in Figure 5.

The $\beta_{\|p}$ dependence of all three quantities here has the same physical basis: As this parameter increases, the relative strength of the magnetic field decreases and the protons are less tightly bound in their cyclotron orbits. This requires less free energy for instability growth and a slower growth rate to maintain a given rate of pitch angle scattering but permits a greater fraction of magnetic energy to enter the fluctuations.

The result that the proton anisotropy/$\beta_{\|p}$ inverse correlation is essentially independent of the rate at which our simulations are driven confirms our contention that this relationship is a fundamental property of plasmas in which the proton cyclotron anisotropy instability is active. However, the result that the γ_m and ϵ/ϵ_o correlations depend on the normalized cutoff speed suggests that these correlations are of a less fundamental nature, involving a dependence on the rate at which the instability is driven, as well on the local plasma parameters. This suggestion is reinforced by noting that the combination of $\beta_{\|p}$ and the normalized v_{cut} in both equations (10) and (11) is similar to the $\beta_{\|p}{}^{1.5}/(v_{cut}/\sqrt{2}v_p)^2$ combination which appears in equation (8). We regard this suggestion as an interesting hypothesis which can be tested through the use of an inhomogeneous, two-dimensional hybrid simulation model of the sheath or by multi-spacecraft observations such as will be provided by the approaching Cluster mission.

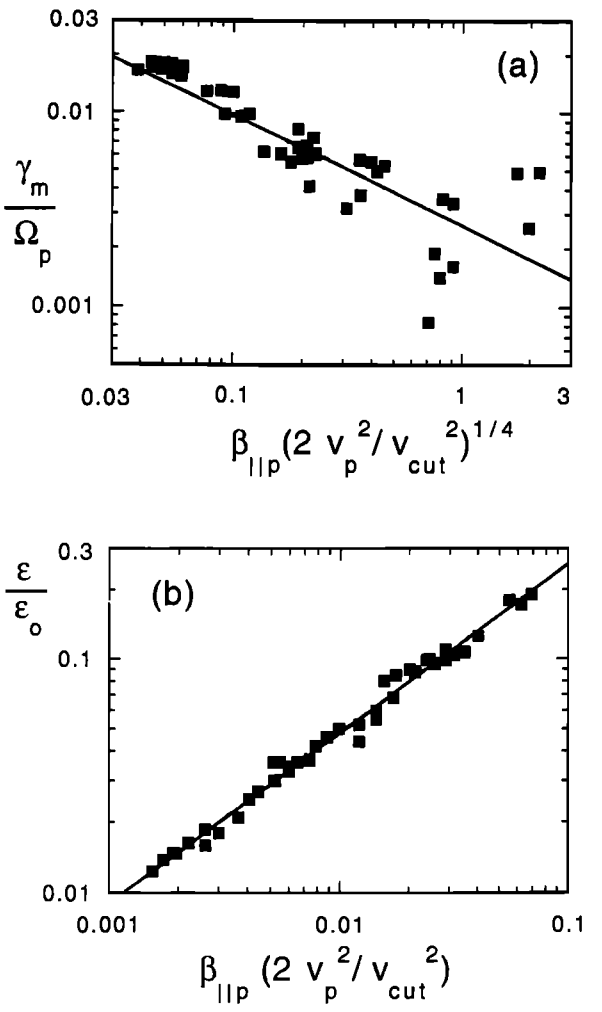

Figure 5. Late-time results from the same ensemble of driven simulations as is described in the caption of Figure 4. (a) The maximum growth rate as a function of $\beta_{\|p}/(v_{cut}/(\sqrt{2}v_p))^{1/2}$. (b) The fluctuating field energy density as a function of $\beta_{\|p}/(v_{cut}/(\sqrt{2}v_p))^2$. The solid lines represent the least squares fits to the results, equation (10) and equation (11), respectively.

It is important to state that neither equation (4) nor equation (9) should be regarded as definitive expressions of the anisotropy/β inverse correlation. This is because we can make weak changes in both the coefficient and the exponent of $\beta_{\|p}$ by including in our ensembles additional simulations which correspond to somewhat different initial conditions, particularly the initial proton anisotropy. One might move toward a more definitive expression by substantially increasing the number of simulations in the ensemble and using a more systematic procedure for choosing initial values for the ensemble members. But, given the relative simplicity of our model, we believe that future work would be more productive if it were directed toward improving the physics of the model rather than merely improving its statistics.

6. Synthesis

We have carried out one-dimensional hybrid computer simulations of the proton cyclotron anisotropy instability to further investigate the role of this growing mode in establishing the inverse correlation between the proton anisotropy and $\beta_{\|p}$ observed in the terrestrial magnetosheath. We have used initial value simulations to emulate the qualitative differences between the CCE and IRM observations in the sheath and have interpreted these differences in terms of plasma parcels that are active or inactive with respect to instability growth.

We also have carried out driven computer simulations in which protons with high magnetic-field-aligned velocities are recycled, modeling the loss of plasma energy (although not the loss of plasma itself) from the subsolar magnetosheath. Our simulations achieve late-time states in which anisotropy increases due to the recycling process are approximately balanced by anisotropy decreases due to wave-particle scattering. These driven simulations yield not only a proton anisotropy/$\beta_{\|p}$ inverse correlation similar to that obtained from our initial value simulations but also scaling expressions for the late-time maximum instability growth rate and fluctuating field energy density. These latter two relations depend not only on $\beta_{\|p}$ but also on the proton recycle frequency, indicating that, unlike the temperature anisotropy, γ_m/Ω_p and ϵ/ϵ_o depend on the strength of the macroscopic driver as well as on the local plasma β.

Equations (10) and (11) are new theoretical results. Because they depend on the rate at which the instability is driven, their detailed form will probably be different for different driven simulation models, so that they are less fundamental relations than the proton anisotropy/$\beta_{\|p}$ correlation. Nevertheless, they both provide useful information. The $\beta_{\|p}$ scaling of equation (11) is commensurate with the observations of *Anderson et al.* [1994] who show $\epsilon/\epsilon_o \sim \beta_{\|p}^{0.5}$ for proton-cyclotron-like fluctuations in their Fig, 9, and the quasilinear theory result of *Gary et al.* [1993b] which predicted $\epsilon/\epsilon_o \sim \beta_{\|p}$ at saturation of initial value simulations of the proton cyclotron instability. Equation (10) states that the late-time simulation results of our model correspond to a maximum growth rate which increases with decreasing $\beta_{\|p}$. This is a more general result than our earlier assumption [*Gary et al.*, 1993c] that the observed anisotropy/β relations may be fit by threshold conditions of constant γ_m. The $\beta_{\|p}$-dependence of equation (10) has the effect of increasing the magnitude of the slope of the proton anisotropy versus $\beta_{\|p}$ curve [compare equation (9) against equations (3)] and implies that full specification of the threshold condition for the terrestrial magnetosheath will require the study of driven simulations of more realistic systems.

7. Limitations and Implications

The simulation model discussed in this manuscript is a simple one and requires further development to resolve the differences between the experimental result of equation (1) and the theoretical/computational threshold of, for example, equation (9). There are many potential sources of these differences: Two important elements which need to be introduced on the theoretical side are a tenuous helium component and a spatially inhomogeneous two-dimensional simulation model. The former effect not only raises the threshold of the proton cyclotron anisotropy instability [*Gary et al.*, 1993a] but also introduces the helium cyclotron anisotropy instability which contributes weak proton scattering [*Denton et al.*, 1993; *Gary and Winske*, 1993]. The use of a two-dimensional simulation model will provide more realistic conditions for the study of this instability and in particular will permit a study of the relationship between the relatively artificial proton recycle model of this manuscript and more physical representations of the macroscopic forces which actually drive proton anisotropies in the magnetosheath.

The results of this manuscript, when coupled with the conclusions of earlier theoretical papers on this subject, imply that, when conditions are appropriate, a logical procedure may be followed to obtain limited closure relations for sufficiently homogeneous, sufficiently anisotropic space plasmas. This procedure is as follows: (1) Use spacecraft observations to demonstrate that an upper bound may be found on some dimensionless parameter which characterizes a plasma anisotropy. (2) Use observations to parameterize the relationship between this bounded parameter and other parameters, local and perhaps global, of the plasma. (3) Use linear Vlasov theory to identify the instability or instabilities associated with this anisotropy and determine the corresponding threshold curve or curves. (4) Use initial value simulations to determine that these instabilities do indeed drive plasma parameters toward their thresholds, and establish which instabilities are most effective at doing this. (5) Use driven simulations to represent the process or processes sustaining the anisotropy, and determine the relationship between the sustained instability growth rate and relevant microscopic and, if appropriate, macroscopic parameters. (6) Observe that the threshold condition corresponding to this prescription for γ_m represents the desired parametric bound for the limited closure relation.

We have applied this procedure to a model based on data from the highly compressed, subsolar magnetosheath downstream of the quasi-perpendicular bow shock. Because it is based on a local theory of relatively short-wavelength instabilities, it is likely that this procedure also may be applied to the terrestrial sheath under more general conditions and indeed to any sufficiently homogeneous space plasmas in which the ions are well described by bi-Maxwellian velocity distributions and which bear a sufficiently large $T_{\perp p}/T_{\|p} > 1$. Such plasma regimes might include the terrestrial magnetosphere [*Lui and Hamilton*, 1992; *Anderson and Hamilton*, 1993], the plasma sheet of Earth's magnetotail [*Nötzel et al.*, 1985], high-speed streams of the solar wind [*Marsch et al.*, 1982], and other planetary magnetosheaths [*Barbosa*, 1993; *Tsurutani et al.*, 1993].

Furthermore, this procedure may also apply to electron temperature anisotropies. The threshold condition for the whistler anisotropy instability [*Gary and Madland*, 1985] is very similar to that of the ion cyclotron anisotropy instability [*Gary et al.*, 1976], implying that under appropriate conditions a similar inverse correlation may exist between the electron temperature anisotropy and the electron parallel β. Since electron anisotropies support growth of the collisionless tearing instability [*Hesse and Winske*, 1993], a limited closure relation for electrons similar to that which we have discussed for ions may also be appropriate for reconnection models.

Even more generally, limited closure due to microinstabilities may hold for different sources of free energy in other space plasma regimes. Possible applications include both electron and ion heat fluxes in the solar wind [e.g., *Feldman et al.*, 1973, 1976], and ion/ion relative flows in the inner magnetosphere [*Winglee et al.*, 1989; *Schriver et al.*, 1990]. Since microinstabilities act within, rather than on, a plasma parcel, they cannot directly alter the average flow speed of that parcel, although they can indirectly change this quantity by limiting the heat flux [*Hollweg*, 1976] or redistributing perpendicular and parallel ion temperatures [*Hesse and Birn*, 1992].

The principles which we have used to obtain limited closure are generally applicable to relatively homogeneous plasmas, and their application to ion anisotropies in the magnetosheath has been relatively straightforward. There are two reasons for this. First, although sheath ion anisotropies drive three distinct instabilities, our simulations have shown that one of these is much more important than the others for determining proton closure. Second, in the sheath the properties of this mode, the proton cyclotron anisotropy instability, and hence the properties of limited closure are largely determined by two dimensionless parameters: $T_{\perp p}/T_{\|p}$ and $\beta_{\|p}$. The presence of helium ions alters the instability threshold [*Gary et al.*, 1993a], but further work on driven instabilities in the presence of a tenuous helium ion component should permit the associated changes to be introduced into equation (9) should such effects become of interest to macroscopic modelers.

For other space plasma regimes the principles of limited closure remain the same, but their application is likely to be less straightforward. Many space plasma regimes exhibit two or more important electron or proton components, so that characterization of these plasmas requires more than two parameters and often involves more than a single dominant instability. So closure may not be a simple two-parameter correlation like equations (1) or (9) but may be a complex mixture of several different threshold expressions. Thus it may be harder to find other limited closure relations in the data, and it will likely be more difficult to establish the theoretical and simulation properties of the instability thresholds. Nevertheless, the threshold approach to wave-particle transport offers a relatively easier path to useful expressions than the alternate procedure of calculating transport coefficients via quasilinear theory, and we strongly recommend it to space plasma modelers who wish to include wave-particle consequences in their large-scale simulations.

The results of *Denton et al.* [1994b] demonstrate that a limited closure relation for the proton temperature anisotropy is necessary to yield good agreement between fluid models and spacecraft observations of perpendicular and parallel proton temperatures in the magnetosheath. But, more generally, would application of such a limited closure relation improve the predictions of densities, flow speeds, and average temperatures by a fluid model of the magnetosheath as compared with observations?

A full answer to this question can only be provided by the application of closure to an anisotropic fluid model of the sheath. Although such an application has not yet been carried out, there are two pieces of evidence that an affirmative answer might be given to the above question. First, *Chen et al.* [1993] have shown that the usual gas-dynamic approximation is inaccurate and that, at least under some circumstances, an MHD code which self-consistently incorporates magnetic field effects is necessary to provide a proper prediction of relatively high-speed magnetosheath flows on the flanks of the magnetosphere. Because these flows are accelerated by the tension in magnetic field lines draped over the nose of the magnetosphere, and because *Denton et al.* [1994b] have shown that temperature anisotropy is closely associated with such draping, it is possible that there is a link between the limited closure relation for this anisotropy and the prediction of flow speeds. Second, *Hesse and Birn* [1992] have tested various expressions for temperature anisotropy closure in their anisotropic fluid model of the magnetotail. Although their closure relations are different in form from the limited closure discussed here, their results clearly show that the manner in which the perpendicular and parallel plasma temperatures are coupled affects the growth rate of the ion tearing instability and, consequently, the flow velocities and magnetic field patterns predicted by their simulations.

Acknowledgments. The Los Alamos portion of this work was performed under the auspices of the U.S. Department of Energy (DOE) and was supported by the DOE Office of Basic Energy Sciences, Division of Engineering and Geosciences, and the Space Plasma Theory Program of the National Aeronautics and Space Administration (NASA). The Dartmouth College portion of this work was supported with funding from NASA grants NAGW-1652 and NAGW-3052-1992. Research at Lockheed was funded through NASA contract NAS5-30565. Work at the Johns Hopkins University Applied Physics Laboratory was supported by NASA under the AMPTE Missions Operations and Data Analysis program.

The Editor thanks S. Schwartz and M. Ashour-Abdalla for their assistance in evaluating this paper.

References

Ambrosiano, J., and S. H. Brecht, A simulation study of the Alfvén ion-cyclotron instability in high-beta plasmas, *Phys. Fluids*, *30*, 108, 1987.

Anderson, B. J., Magnetic spectral and plasma signatures in the magnetosheath, *Eos Trans. AGU*, *74*(16), Spring Meeting suppl., 273, 1993.

Anderson, B. J., and S. A. Fuselier, Magnetic pulsations from 0.1 to 4.0 Hz and associated plasma properties in the Earth's subsolar magnetosheath and plasma depletion layer, *J. Geophys. Res.*, *98*, 1461, 1993.

Anderson, B. J., and D. C. Hamilton, Electromagnetic ion cyclotron waves stimulated by modest magnetospheric compressions, *J. Geophys. Res.*, *98*, 11,369, 1993.

Anderson, B. J., S. A. Fuselier, and D. Murr, Electromag-

netic ion cyclotron waves observed in the plasma depletion layer, *Geophys. Res. Lett.*, *18*, 1955, 1991.

Anderson, B. J., S. A. Fuselier, S. P. Gary and R. E. Denton, Magnetic spectral signatures in the Earth's magnetosheath and plasma depletion layer, *J. Geophys. Res.*, *99*, in press, 1994.

Barbosa, D. D., Theory and observations of electromagnetic ion cyclotron waves in Saturn's inner magnetosphere, *J. Geophys. Res.*, *98*, 9345, 1993.

Brinca, A. L., N. Sckopke, and G. Paschmann, Wave excitation downstream of the low-β, quasi-perpendicular bow shock, *J. Geophys. Res.*, *95*, 6331, 1990.

Chen, S.-H., M. G. Kivelson, J. T. Gosling, R. J. Walker, and A. J. Lazarus, Anomalous aspects of magnetosheath flow and of the shape and oscillations of the magnetopause during an interval of strongly northward interplanetary magnetic field, *J. Geophys. Res.*, *98*, 5727, 1993.

Dendy, R. O., and K. G. McClements, Ion cyclotron wave emission at the quasi-perpendicular bow shock, *J. Geophys. Res.*, *98*, 15,531, 1993.

Denton, R. E., M. K. Hudson, S. A. Fuselier, and B. J. Anderson, Electromagnetic ion cyclotron waves in the magnetosheath plasma depletion layer, *J. Geophys. Res.*, *98*, 13,477, 1993.

Denton, R. E., S. P. Gary, B. J. Anderson, S. A. Fuselier, and M. K. Hudson, Low-frequency magnetic fluctuation spectra in the magnetosheath and plasma depletion layer, *J. Geophys. Res.*, *99*, in press, 1994a.

Denton, R. E., B. J. Anderson, S. P. Gary, and S. A. Fuselier, Bounded anisotropy fluid model, *J. Geophys. Res.*, submitted, 1994b.

Farris, M. H., C. T. Russell, and M. F. Thomsen, Magnetic structure of the low beta, quasi-perpendicular shock, *J. Geophys. Res.*, *98*, 15,285, 1993.

Feldman, W. C., J. R. Asbridge, S. J. Bame, and H. R. Lewis, Empirical closure relation for the Vlasov moment equations, *Phys. Rev. Lett.*, *30*, 271, 1973.

Feldman, W. C., J. R. Asbridge, S. J. Bame, S. P. Gary, and M. D. Montgomery, Electron parameter correlations in high-speed streams and heat flux instabilities, *J. Geophys. Res.*, *81*, 2377, 1976.

Fuselier, S. A., D. M. Klumpar, and E. G. Shelley, On the origins of energetic ions in the Earth's dayside magnetosheath, *J. Geophys. Res.*, *96*, 47, 1991a.

Fuselier, S. A., D. M. Klumpar, E. G. Shelley, B. J. Anderson, and A. J. Coates, He^{2+} and H^+ dynamics in the subsolar magnetosheath and plasma depletion layer, *J. Geophys. Res.*, *96*, 21,095, 1991b.

Gary, S. P., Wave-particle transport from electrostatic instabilities, *Phys. Fluids*, *23*, 1193, 1980.

Gary, S. P., *Theory of Space Plasma Microinstabilities*, Cambridge University Press, New York, 1993.

Gary, S. P., and C. D. Madland, Electromagnetic electron temperature anisotropy instabilities, *J. Geophys. Res.*, *90*, 7607, 1985.

Gary, S. P., and D. Winske, Simulations of ion cyclotron anisotropy instabilities in the terrestrial magnetosheath, *J. Geophys. Res.*, *98*, 9171, 1993.

Gary, S. P., M. D. Montgomery, W. C. Feldman, and D. W. Forslund, Proton temperature anisotropy instabilities in the solar wind, *J. Geophys. Res.*, *81*, 1241, 1976.

Gary, S. P., S. A. Fuselier, and B. J. Anderson, Ion anisotropy instabilities in the magnetosheath, *J. Geophys. Res.*, *98*, 1481, 1993a.

Gary, S. P., M. E. McKean, and D. Winske, Ion cyclotron anisotropy instabilities in the magnetosheath: theory and simulations, *J. Geophys. Res.*, *98*, 3963, 1993b.

Gary, S. P., B. J. Anderson, R. E. Denton, S. A. Fuselier, M. E. McKean, and D. Winske, Ion anisotropies in the magnetosheath, *Geophys. Res. Lett.*, *20*, 1767, 1993c.

Hau, L.-N., T.-D. Phan, B. U. Ö. Sonnerup, and G. Paschmann, Double-polytropic closure in the magnetosheath, *Geophys. Res. Lett.*, *20*, 2255, 1993.

Hesse, M., and J. Birn, MHD modeling of magnetotail instability for anisotropic pressure, *J. Geophys. Res.*, *97*, 10,643, 1992.

Hesse, M., and D. Winske, Hybrid simulations of collisionless ion tearing, *Geophys. Res. Lett.*, *20*, 1207, 1993.

Hollweg, J. V., Collisionless electron heat conduction in the solar wind, *J. Geophys. Res.*, *81*, 1649, 1976.

Lacombe, C., F. G. E. Pantellini, D. Hubert, C. C. Harvey, A. Mangeney, G. Belmont, and C. T. Russell, Mirror and Alfvénic waves observed by ISEE 1-2 during crossings of the Earth's bow shock, *Ann. Geophys.*, *10*, 772, 1992.

Lui, A. T. Y., and D. C. Hamilton, Radial profiles of quiet time magnetospheric parameters, *J. Geophys. Res.*, *97*, 19,325, 1992.

Manheimer, W., and J. P. Boris, Marginal stability analysis–A simpler approach to anomalous transport in plasmas, *Comments Plasma Phys. Controlled Fusion*, *3*, 15, 1977.

Marsch, E., K.-H. Muhlhauser, R. Schwenn, H. Rosenbauer, W. Pilipp, and F. M. Neubauer, Solar wind protons: Three-dimensional velocity distributions and derived plasma parameters measured between 0.3 and 1 AU, *J. Geophys. Res.*, *87*, 52, 1982.

McKean, M. E., D. Winske, and S. P. Gary, Kinetic properties of mirror waves in magnetosheath plasmas, *Geophys. Res. Lett.*, *19*, 1331, 1992a.

McKean, M. E., D. Winske, and S. P. Gary, Mirror and ion cyclotron anisotropy instabilities in the magnetosheath, *J. Geophys. Res.*, *97*, 19,421, 1992b.

McKean, M. E., D. Winske, and S. P. Gary, Two-dimensional simulations of ion anisotropy instabilities in the magnetosheath, *J. Geophys. Res.*, *99*, in press, 1994.

Nötzel, A., K. Schindler, and J. Birn, On the cause of approximate pressure isotropy in the quiet near-Earth plasma sheet, *J. Geophys. Res.*, *90*, 8293, 1985.

Paschmann, G., W. Baumjohann, N. Sckopke, T.-D. Phan, and H. Lühr, Structure of the dayside magnetopause for low magnetic shear, *J. Geophys. Res.*, *98*, 13,409, 1993.

Phan, T.-D., G. Paschmann, W. Baumjohann, and N. Sckopke, The magnetosheath region adjacent to the dayside magnetopause: AMPTE/IRM observations, *J. Geophys. Res.*, *99*, 121, 1994.

Schriver, D., M. Ashour-Abdalla, H. Collin, and N. Lallande, Ion beam heating in the auroral zone, *J. Geophys. Res.*, *95*, 1015, 1990.

Sckopke, N., G. Paschmann, A. L. Brinca, C. W. Carlson, and H. Lühr, Ion thermalization in quasi-perpendicular shocks involving reflected ions, *J. Geophys. Res.*, *95*, 6337, 1990.

Song, P., R. C. Elphic, C. T. Russell, J. T. Gosling, and C. A. Cattell, Structure and properties of the subsolar magnetopause for northward IMF: ISEE observations, *J. Geophys. Res.*, *95*, 6375, 1990.

Song, P., C. T. Russell, and M. F. Thomsen, Waves in the in-

ner magnetosheath: A case study, *Geophys. Res. Lett.*, *19*, 2191, 1992.

Song, P., C. T. Russell, and C. Y. Huang, Wave properties near the subsolar magnetopause: Pc 1 waves in the sheath transition layer, *J. Geophys. Res.*, *98*, 5907, 1993.

Takahashi, K., D. G. Sibeck, P. T. Newell, and H. E. Spence, ULF waves in the low-latitude boundary layer and their relationship to magnetospheric pulsations: A multisatellite observation, *J. Geophys. Res.*, *96*, 9503, 1991.

Tsurutani, B. T., E. J. Smith, R. R. Anderson, K. W. Ogilvie, J. D. Scudder, D. N. Baker, and S. J. Bame, Lion roars and nonoscillatory drift mirror waves in the magnetosheath, *J. Geophys. Res.*, *87*, 6060, 1982.

Tsurutani, B. T., D. J. Southwood, E. J. Smith, and A. Balogh, A survey of low frequency waves at Jupiter: The Ulysses encounter, *J. Geophys. Res.*, *98*, 21,203, 1993.

Winglee, R. M., P. B. Dusenbery, H. L. Collin, C. S. Lin, and A. M. Persoon, Simulations and observations of heating of auroral ion beams, *J. Geophys. Res.*, *94*, 8943, 1989.

Winske, D., and N. Omidi, Hybrid codes: Methods and applications, in *Computer Space Plasma Physics: Simulation Techniques and Software*, edited by H. Matsumoto and Y. Omura, p. 103, Terra Scientific Publishers, Tokyo, 1993.

B. J. Anderson, Applied Physics Laboratory, Johns Hopkins University, Johns Hopkins Road, Laurel, MD 20723-6099. (Internet e-mail: anderson@ampte.dnet.nasa.gov)

R. E. Denton, Department of Physics and Astronomy, Dartmouth College, 6127 Wilder Laboratory, Hanover, NH 03755-3528 (Internet e-mail: denton@comet.dartmouth.edu)

S. A. Fuselier, Department 91-20, Building 225, Lockheed Palo Alto Research Laboratory, 3251 Hanover Street, Palo Alto, CA 94304-1191 (Internet e-mail: fuselier@lockhd.-dnet.nasa.gov)

S. P. Gary, M. S. D466, Los Alamos National Laboratory, Los Alamos, NM 87545 (Internet e-mail: pgary@lanl.gov)

M. E. McKean, Department of ECE, University of California, San Diego, La Jolla, CA 92093-0407. (Internet e-mail: mmckean@ece.ucsd.edu)

D. Winske, M. S. F645, Los Alamos National Laboratory, Los Alamos, NM 87545 (Internet e-mail: dw@demos.lanl.-gov)

(Received July 13, 1993; revised October 26, 1993; accepted December 16, 1993.)